RESEARCH ARTICLE

National Science Review
9: nwac106, 2022
https://doi.org/10.1093/nsr/nwac106
Advance access publication 3 June 2022

EARTH SCIENCES

Isotopic constraints confirm the significant role of microbial nitrogen oxides emissions from the land and ocean environment

Wei Song[1], Xue-Yan Liu[1,*], Benjamin Z. Houlton[2] and Cong-Qiang Liu[1]

ABSTRACT

Nitrogen oxides (NO_x, the sum of nitric oxide (NO) and N dioxide (NO_2)) emissions and deposition have increased markedly over the past several decades, resulting in many adverse outcomes in both terrestrial and oceanic environments. However, because the microbial NO_x emissions have been substantially underestimated on the land and unconstrained in the ocean, the global microbial NO_x emissions and their importance relative to the known fossil-fuel NO_x emissions remain unclear. Here we complied data on stable N isotopes of nitrate in atmospheric particulates over the land and ocean to ground-truth estimates of NO_x emissions worldwide. By considering the N isotope effect of NO_x transformations to particulate nitrate combined with dominant NO_x emissions in the land (coal combustion, oil combustion, biomass burning and microbial N cycle) and ocean (oil combustion, microbial N cycle), we demonstrated that microbial NO_x emissions account for 24 ± 4%, 58 ± 3% and 31 ± 12% in the land, ocean and global environment, respectively. Corresponding amounts of microbial NO_x emissions in the land (13.6 ± 4.7 Tg N yr^{-1}), ocean (8.8 ± 1.5 Tg N yr^{-1}) and globe (22.5 ± 4.7 Tg N yr^{-1}) are about 0.5, 1.4 and 0.6 times on average those of fossil-fuel NO_x emissions in these sectors. Our findings provide empirical constraints on model predictions, revealing significant contributions of the microbial N cycle to regional NO_x emissions into the atmospheric system, which is critical information for mitigating strategies, budgeting N deposition and evaluating the effects of atmospheric NO_x loading on the world.

Keywords: nitrogen isotopes, nitrate, NO_x emission, nitrogen deposition, microbial N cycle

[1]School of Earth System Science, Tianjin University, Tianjin 300072, China and [2]Department of Global Development and Department of Ecology and Evolutionary Biology, Cornell University, Ithaca, NY 14850, USA

***Corresponding author.** E-mail: liuxueyan@tju.edu.cn

Received 18 May 2022; **Revised** 28 May 2022; **Accepted** 31 May 2022

INTRODUCTION

Atmospheric nitrogen oxides (NO_x) loading influence human health (e.g. respiratory and cardiovascular diseases, acute bronchitis) [1], tropospheric chemistry (e.g. precipitation acidity, aerosol and ozone formation) [2–4], climate [4] and economic development [5]. In past decades, anthropogenic NO_x emissions have significantly increased the fluxes of atmospheric NO_3^- deposition [6–8], altered N cycles in both terrestrial and marine ecosystems [9–12] and thus affected microbial NO_x emissions to the atmosphere [13]. Hence, it is pivotal to accurately constrain land and ocean NO_x emissions to the atmosphere to mitigate human-induced NO_x emissions, budget NO_3^- deposition fluxes and evaluate the eco-environmental and climatic effects of atmospheric NO_x loading. However, it has long been challenging to accurately constrain land- and ocean-to-atmosphere NO_x emissions due to uncertainties over microbial N cycles in both land and ocean.

In marine environments, the oil combustion of marine traffic transportation is a known source of NO_x emissions [14–20]. According to the European Monitoring and Evaluation Programme Meteorological Synthesizing Centre West model, NO_x emissions from oil combustion in the ocean averaged 6.4 ± 0.8 Tg N yr^{-1} (5.0–7.8 Tg N yr^{-1}) [14–20]. However, the microbial N cycle occurring in the ocean is the other significant source of NO_x emissions [21–24]. First, earlier studies based on molecular analysis and lab culture experiments have confirmed that multiple kinds of bacteria associated with several processes of microbial N cycles

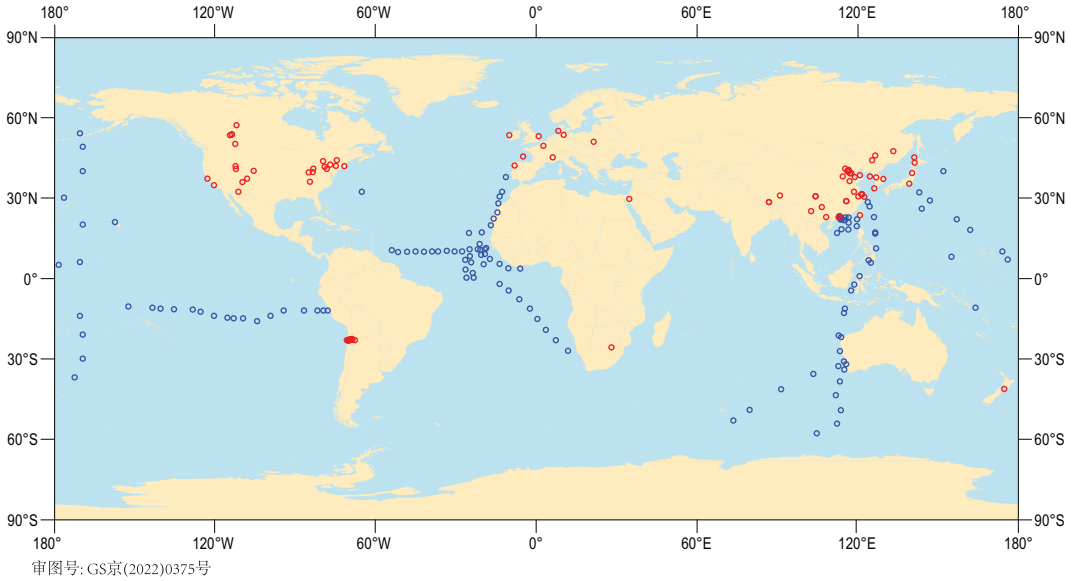

Figure 1. The distribution of study sites with $\delta^{15}N_{p\text{-}N03\text{-}}$ observations. Red and blue circles represent land sites ($n = 91$) and ocean sites ($n = 134$), respectively.

can produce NO, e.g. ammonium-oxidizing bacteria, nitrite-oxidizing bacteria, methanotrophic bacteria and denitrifying bacteria [25–29]. Second, nitrification in the oxic layer of the ocean is a significant source of NO [22] and NO can be produced in biofilms and marine sediments [30]. Third, *Ulva prolifera* (forming a belt on a vertical concrete wall in the upper intertidal zone at low tide) was the primary contributor to the high NO concentrations during the late-bloom period [31]. Meanwhile, the photolysis of NO_2^- and NO_3^- (in the surface water and on particles) or alkyl nitrates or dissolved organic matter may also be the sources of atmospheric NO in the ocean [32–35]. However, due to its high reactivity [36], NO would be involved quickly into the NO_x cycle in the atmosphere [34]. Accordingly, it has long been difficult to accurately observe microbial NO emissions in the ocean [24]. Until now, microbial NO_x emissions from the ocean and their fractional contribution to total NO_x emissions from the ocean have not been quantified [21–24]. Hitherto, owing to the lack of microbial NO_x emissions, the NO_x from oil combustion has long been assumed as the total ocean NO_x emissions in reports of the Intergovernmental Panel on Climate Change (IPCC) [20].

In the land environment, NO_x emissions are mainly derived from coal combustion, oil combustion, biomass burning and microbial N cycles in substrates such as waters, soils and wastes [3,37–40]. Currently, emission amounts of NO_x from coal combustion [10,41], oil combustion [42] and biomass burning [43,44] have been reported explicitly in national statistic yearbooks and emission inventories [45–47]. However, land NO_x emissions from microbial N cycles have been observed chiefly for soils under natural vegetation and agriculture [40,43,48]. Therefore, estimates of NO_x emissions from the land are based on limited empirical observations combined with process and statistical models and satellites used to scale up emissions [40,49,50]. Based on IPCC reports, microbial NO_x emissions were budgeted at 5.6 Tg N yr^{-1} before 2001, increasing to 11.0 Tg N yr^{-1} when incorporating more observational data in the report of 2013 [40,49,50]. This doubling of emissions highlights a substantial underestimation of microbial NO_x emissions in the land, which has shifted with additional measurements and better models. New methods are strongly needed to comprehensively constrain microbial NO_x emissions from soils and many other unconsidered substrates (such as the surface water of rivers, lakes, swamps, etc.) and emission sources (such as wastewater, water treatment systems, solid wastes).

Here we provided a unique evaluation of the relative importance of the microbial NO_x emissions in the land and ocean to the known fossil-fuel NO_x emissions and then made a new budget for global microbial NO_x emissions. First, we compiled stable N isotopes ($\delta^{15}N$ values) of NO_3^- in atmospheric particulates (denoted as $\delta^{15}N_{p\text{-}NO3\text{-}}$ hereafter) in the land and ocean, respectively (detailed in 'Materials and methods' section) (Fig. 1 and Supplementary Table S1). Second, based on concentrations and $\delta^{15}N$ of NO_x, HNO_3 and p-NO_3^- over the land, we estimated the $\delta^{15}N$ of the initial NO_x mixture from different emission sources in the atmosphere (denoted as $\delta^{15}N_{i\text{-}NOx}$, Supplementary Fig. S1) and the

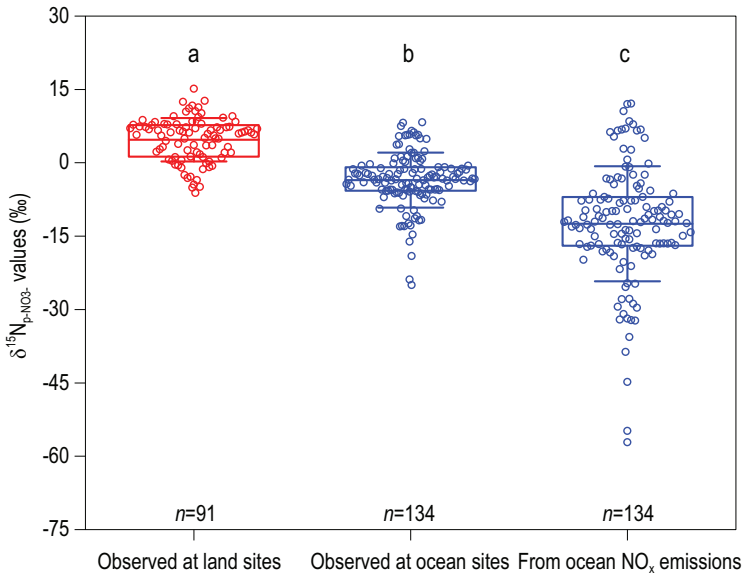

Figure 2. $\delta^{15}N_{p\text{-}NO3\text{-}}$ values observed at land sites, observed at ocean sites and derived from ocean NO_x emissions. Circles around each box show mean values of replicate measurements at each site (*n*) (replicate measurements at each site are 1—318 and 1—72 for land and ocean sites, respectively). The box encompasses the 25th to 75th percentiles; whiskers and lines in boxes are the SD and mean values, respectively. Different letters above the boxes show significant differences at $P < 0.05$.

difference between $\delta^{15}N_{p\text{-}NO3\text{-}}$ and $\delta^{15}N_{i\text{-}NOx}$ values (denoted as $^{15}\Delta_{i\text{-}NOx\rightarrow p\text{-}NO3\text{-}}$) (detailed in 'Materials and methods' section). By using $^{15}\Delta_{i\text{-}NOx\rightarrow p\text{-}NO3\text{-}}$ (Supplementary Fig. S2), $\delta^{15}N_{p\text{-}NO3\text{-}}$ (Fig. 2) and $\delta^{15}N$ of dominant sources of NO_x emissions (coal combustion, oil combustion, biomass burning and microbial N cycles, Supplementary Table S2), we estimated the relative contributions of dominant NO_x sources from the land and ocean, respectively, by developing a model of Stable Isotope Analysis in R code (detailed in 'Materials and methods' section). Finally, combining fractional contributions with corresponding amounts of fossil-fuel NO_x emissions from the land and the ocean, we calculated the amount of microbial NO_x emissions in the land and ocean, respectively (detailed in 'Materials and methods' section).

RESULTS AND DISCUSSION

Different $\delta^{15}N$ signatures of atmospheric p-NO_3^- between the land and ocean

Mean $\delta^{15}N_{p\text{-}NO3\text{-}}$ observed over terrestrial sites (4.7 ± 3.6‰; $n = 91$) was significantly higher ($p < 0.05$) than that observed for ocean sites (−3.5 ± 3.9‰; $n = 134$) (Fig. 2). This finding implied that human activities contributed relatively more ^{15}N-enriched NO_x to atmospheric NO_x loading on the land than in the ocean.

First, the $\delta^{15}N_{p\text{-}NO3\text{-}}$ signal observed at land sites can represent land NO_x emissions without a significant overprinting of marine sources. The net water vapor flux transported from the ocean to the land accounted for only 10% of the total water evaporation over the ocean [51,52]. According to the existing oceanic NO_x emissions (6.4 ± 0.8 Tg N yr^{-1} based on the known oil combustion) [14–20] and the land NO_x emissions (53.3 ± 4.6 Tg N yr^{-1}) [43,53–58], the ocean-to-land atmospheric transport of NO_x accounts for only 1.2% of land NO_x emissions and thus is often assumed negligible [35]. Accordingly, the $\delta^{15}N_{p\text{-}NO3\text{-}}$ values observed at land sites can be directly used to differentiate dominant sources of NO_x emissions (Equation 5 in the online Supplementary Data).

However, the $\delta^{15}N_{p\text{-}NO3\text{-}}$ signal observed at ocean sites cannot represent the NO_3^- purely derived from ocean NO_x emissions. Because the land has much higher NO_x emissions and a smaller area, and thus a higher concentration than the ocean [57,59,60], the net transportation of atmospheric NO_x occurs from the land to the ocean. The modeled NO_y (the sum of NO_x, inorganic and organic nitrates in the atmosphere) transportation (11.0 Tg N yr^{-1}) [61] is about 1.7 times the oceanic and accounts for 21% of land NO_x emissions. Accordingly, the $\delta^{15}N$ signals of p-NO_3^- derived from the land-to-ocean NO_y transportation should be excluded (Equation 2 in the online Supplementary Data) to obtain the $\delta^{15}N$ values of p-NO_3^- derived only from the ocean NO_x emissions (Supplementary Fig. S1) to differentiate the relative contributions between oil combustion and microbial NO_x emissions (Equation 6 in the online Supplementary Data). Besides, the land-derived NO_x and p-NO_3^- are the dominant form of the land-to-ocean NO_y transportation and between them, the p-NO_3^- is the main type to be transported because the lifetime of NO_x is much shorter [35,61,62]. So far, no substantial isotope effect was assumed for the physical processes of atmospheric transportation [63,64]. Thus, we thought that the ocean p-NO_3^- produced by the land-derived NO_x did not differ isotopically from the land p-NO_3^- and used isotope mass-balance calculations to obtain the $\delta^{15}N$ values of p-NO_3^- derived only from the ocean NO_x emissions (Equation 2 in the online Supplementary Data).

The calculated results revealed that the $\delta^{15}N$ of p-NO_3^- purely derived from ocean NO_x emissions averaged −12.5 ± 8.2‰ (Fig. 2), which was much lower than the $\delta^{15}N_{p\text{-}NO3\text{-}}$ observed for the land sites (4.7 ± 3.6‰; Fig. 2). The increase in $^{15}N/^{14}N$ of p-NO_3^- over the land should be mainly influenced by ^{15}N-enriched NO_x sourced to coal combustion, which was distinctly elevated in $\delta^{15}N$

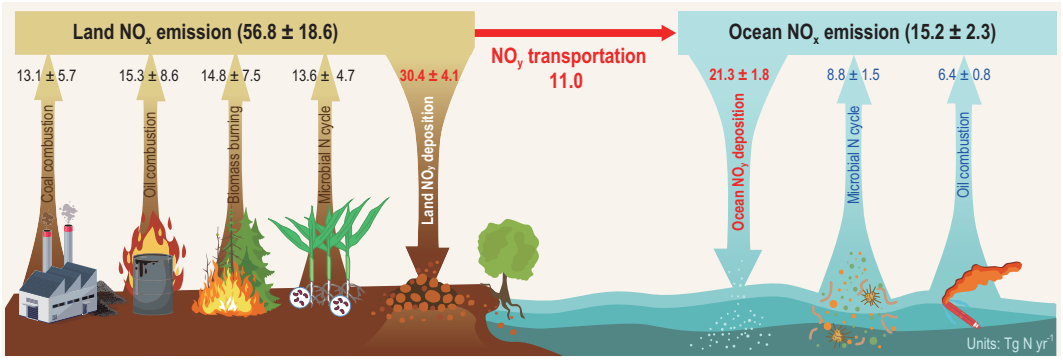

Figure 3. Emissions of significant land and ocean NO_x sources (in black and blue) based on natural isotope methods (detailed in 'Materials and methods' section). Data of the NO_y deposition and transportation (in red) were cited from Refs [35,61,62,70,89,90].

values (mean = 14.2 ± 5.1‰, Supplementary Table S2). However, the lower $^{15}N/^{14}N$ of p-NO_3^- derived from ocean NO_x emissions revealed a microbial NO_x source with distinctly lower $\delta^{15}N$ values than other sources (mean = −37.0 ± 13.5‰, Supplementary Table S2). Our findings demonstrated the contrasting $\delta^{15}N$ pattern between p-NO_3^- derived from the land and ocean NO_x emissions. Moreover, the newly constrained $\delta^{15}N$ of p-NO_3^- sourced to ocean NO_x emissions provided a more accurate and straightforward opportunity to constrain source contributions and emission amounts via isotope modeling.

Relative contributions of dominant NO_x sources to p-NO_3^-

$\delta^{15}N_{p\text{-}NO3\text{-}}$ values are determined by the $\delta^{15}N$ of sources and their relative contributions to total NO_x emission and isotope effects of the NO_x transformation to p-NO_3^- ($^{15}\Delta_{i\text{-}NOx\rightarrow p\text{-}NO3\text{-}}$ values) [65]. Accordingly, we compiled $\delta^{15}N$ values of dominant sources of NO_x emissions (Supplementary Table S2), constrained $^{15}\Delta_{i\text{-}NOx\rightarrow p\text{-}NO3\text{-}}$ values (Supplementary Fig. S2) and thereby constructed isotope mass-balance models to further evaluate the contribution of dominant NO_x sources to p-NO_3^- in the land and ocean, respectively (detailed in 'Materials and methods' section).

For source $\delta^{15}N$ end-members, we considered coal combustion, oil combustion, biomass burning and the microbial N cycle as dominant NO_x sources of p-NO_3^- over the land [65], while oil combustion and the microbial N cycle are dominant NO_x sources to p-NO_3^- over the ocean [2,20]. The $\delta^{15}N$ of such sources differ significantly from each other ($p < 0.05$, Supplementary Table S2), which is a prerequisite to differentiating their relative contributions isotopically. We assumed the same $\delta^{15}N$ value of each NO_x source for both land and ocean sites due to no $\delta^{15}N$ observations on NO_x from oil combustion and microbial N cycle in the ocean (detailed in 'Materials and methods' section). We did not consider lightning a dominant NO_x source because the NO_x produced by lightning in the land and ocean atmosphere is negligible. First, the global NO_x production from lighting is 5.2 ± 1.0 Tg N yr^{-1} (Supplementary Text S1), which accounted for ∼9.7% and ∼7.2% of global NO_x emissions by modeling methods (51.9–58.0 Tg N yr^{-1}) and by isotopic methods in this study (Fig. 3). Moreover, the meridional distribution of global lightning in the atmosphere shows three main lightning centers of the Americas, Africa and the maritime continent in Southeast Asia. The minima represent the oceanic regions where little lightning is observed [66]. This baseline assumption of the dominant NO_x sources is supported by emission inventory and deposition modeling [10,41,42,45–47].

Regarding isotope effects, we estimated $^{15}\Delta_{i\text{-}NOx\rightarrow p\text{-}NO3\text{-}}$ values under two independent scenarios (detailed in 'Materials and methods' section) and found no significant differences between them (11.3 ± 2.1‰ and 13.1 ± 3.8‰, respectively) (Supplementary Fig. S2). Accordingly, we used the mean $^{15}\Delta_{i\text{-}NOx\rightarrow p\text{-}NO3\text{-}}$ estimate (12.2 ± 2.2‰) in our subsequent isotope mass-balance calculations (Supplementary Fig. S2). The mean $^{15}\Delta_{i\text{-}NOx\rightarrow p\text{-}NO3\text{-}}$ value in this study (12.2 ± 2.2‰) did not differ from the $\varepsilon_{NO\rightarrow p\text{-}NO3\text{-}}$ value estimated by Li *et al.* [67] (∼15‰) and was also comparable with the global mean $^{15}\Delta_{i\text{-}NOx\rightarrow p\text{-}NO3\text{-}}$ value (16.7 ± 2.3‰) [65]. The calculation of the global mean $^{15}\Delta_{i\text{-}NOx\rightarrow p\text{-}NO3\text{-}}$ value by Song *et al.* [65] was based on the theoretical framework of computation established by Walters and Michalski [68,69], which combined natural ^{15}N and ^{17}O isotopes with environmental parameters relating to the NO_x oxidization to p-NO_3^-. Relative contributions of dominant NO_x sources

were calculated using the Stable Isotope Analysis model in R programming language (detailed in 'Materials and methods' section). Results showed that the NO_x from coal combustion, oil combustion, biomass burning and microbial N cycle accounted for 23 ± 7%, 27 ± 11%, 26 ± 10% and 24 ± 4% on the land, respectively (Supplementary Fig. S3a). In contrast, the NO_x from oil combustion and microbial N cycle accounted for 42 ± 3% and 58 ± 3% in the ocean, respectively (Supplementary Fig. S3a). Generally, high fractions of microbial NO_x emissions revealed the vital contribution of this pathway to both land and ocean NO_x emissions into the global atmosphere.

Total and microbial NO_x emissions on the land

Based on statistical data on quantities and NO_x emission factors of coal and oil combustions in the land system, previous studies have estimated global fossil-fuel NO_x emissions with a relatively high degree of certainty [7,43,50,70,71]. Global fossil-fuel NO_x emissions averaged 28.4 ± 1.8 Tg N yr^{-1}, showing a relatively low variation over past decades (25.6–30.0 Tg N yr^{-1}) [7,43,50,70,71]. By using the fraction and amount of fossil-fuel NO_x emissions in the land (50 ± 14% and 28.4 ± 1.8 Tg N yr^{-1}, respectively, Supplementary Fig. S3a), we estimated that total land NO_x emissions were 56.8 ± 18.6 Tg N yr^{-1} (Fig. 3 and Supplementary Fig. S3b). Our estimate falls in the range of the total land NO_x emissions (50.0–61.4 Tg N yr^{-1}; averaging 55.6 ± 2.9 Tg N yr^{-1}) estimated by optimized modeling methods by considering more microbial sources of NO_x emissions [54,57,58]. However, our estimate is higher than the total land NO_x emissions (39.7–51.0 Tg N yr^{-1}; averaging 43.8 ± 5.0 Tg N yr^{-1}) estimated using the global NO_2 satellite column concentrations [43,55,56]. Due to no consideration of the influences of atmospheric NO_2 transformations, the estimates based on the satellite data were thought to underestimate global NO_x emissions [72–74].

Based on the fraction and amount of total land NO_x emissions (24 ± 4% and 56.8 ± 18.6 Tg N yr^{-1}, respectively, Fig. 3 and Supplementary Fig. S3), microbial NO_x emissions on the land were calculated as 13.6 ± 4.7 Tg N yr^{-1} (Fig. 3 and Supplementary Fig. S3b). So far, observations on microbial NO_x emissions on the land showed a relatively lower flux of 7.9 ± 1.5 Tg N yr^{-1} (5.0–11.0 Tg N yr^{-1}; data compiled from Refs [43,55,75–84]) than our estimate, because these observations have been conducted mainly on fertilized soils and merely on unfertilized soils and other land substrates. Besides, few modeling studies showed distinctly higher fluxes of land microbial NO_x emissions ≤20.4 Tg N yr^{-1} [80] and 23.6 Tg N yr^{-1} [85] than the observation results and our estimate, due to overestimated N inputs in cropland and natural ecosystems and largely overlooked the influence of NO_x sink uncertainties on the satellite-derived NO_x fluxes. However, by considering more substrates of microbial N cycles on the land to optimize the modeling methods, some studies showed the land microbial NO_x emissions as 11.5–13.6 Tg N yr^{-1} (12.4 ± 0.7 Tg N yr^{-1}) [53,71,86,87], which is very comparable with our estimate. The isotopic method in our study offers a comprehensive and accurate constraining on microbial NO_x emissions.

Total and microbial NO_x emissions in the ocean

Based on statistical data of quantities and NO_x emission factors of oil combustions in the ocean system, ocean fossil-fuel NO_x emissions have been estimated as 6.4 ± 0.8 Tg N yr^{-1} on average (5.0–7.8 Tg N yr^{-1}; compiled from [14–20]). Using the fraction of the ocean fossil-fuel NO_x emissions in our study (42 ± 3%, Supplementary Fig. S3a), we estimated the total ocean NO_x emissions as 15.2 ± 2.3 Tg N yr^{-1} (Fig. 3 and Supplementary Fig. S3b). The ocean NO_y deposition averaged 21.3 ± 1.8 Tg N yr^{-1} (18.0–23.0 Tg N yr^{-1}; compiled from Refs [35,61,62,88–90]), which includes the land-to-ocean NO_y transportation of 11.0 Tg N yr^{-1} [61]. Accordingly, the oceanic NO_y deposition derived from oceanic NO_x emissions was 10.3 ± 1.8 Tg N yr^{-1}, which is lower than our study's total ocean NO_x emissions. The generally higher NO_x emissions than NO_y deposition in the ocean might be attributed to other fates such as biological NO_x uptake and atmosphere retention. Further, we calculated ocean microbial NO_x emissions as 8.8 ± 1.5 Tg N yr^{-1} on average (Fig. 3 and Supplementary Fig. S3b). Our results updated the total and microbial NO_x emissions in the marine environment.

Total and microbial NO_x emissions in the globe

By integrating the land and ocean values together (detailed in 'Materials and methods' section), we calculated global total NO_x emissions as 72.0 ± 18.1 Tg N yr^{-1} (Fig. 3 and Supplementary Fig. S3b). Before this work, the modeled total land

NO_x emissions (39.7–61.4 Tg N yr^{-1}; compiled from Refs [43,53–58]) have been assumed as the global NO_x emissions because the ocean NO_x emissions have been unconstrained. Our results showed that oceanic NO_x emissions accounted for ∼21% of the global NO_x emissions. The global NO_x emissions have been underestimated by 15–45% because oceanic NO_x emissions have been unconsidered.

Moreover, we found that microbial NO_x emissions accounted for 31 ± 12% of the total NO_x emissions globally and reached up to 22.5 ± 4.7 Tg N yr^{-1} (Fig. 3 and Supplementary Fig. S3b). By comparison, microbial NO_x emissions in the land (13.6 ± 4.7 Tg N yr^{-1}), ocean (8.8 ± 1.5 Tg N yr^{-1}) and globe (22.5 ± 4.7 Tg N yr^{-1}) are ∼0.5, 1.4 and 0.6 times fossil-fuel NO_x emissions in the land, ocean and globe, respectively (Fig. 3 and Supplementary Fig. S3b). Our results highlight a vital role of the microbial N cycle in global NO_x emissions. In addition to the direct impacts of fossil-fuel combustion on global NO_x emissions, other human activities such as inefficient fertilizer use in cropping systems, wastes and sewage discharge and treatments, N deposition and water N enrichment all can accelerate microbial NO_x emissions in the land, inland water bodies, estuaries and ocean [13,91].

Our results offer an updated and isotopically grounded estimate of land- and ocean-to-atmosphere NO_x emissions. Notably, our results revealed that previous reports have largely underestimated land-based microbial NO_x emissions, constrained long-missing uncertainties over ocean microbial NO_x emissions and therefore elevated the recognition of the substantial contribution of the microbial N cycle to global NO_x emissions. Moreover, our findings highlight the unique significance of natural records of atmospheric N isotopes for understanding global N biogeochemical cycles. Currently, reducing NO_x emissions to alleviate N pollution while sustaining economic development is a major challenge in the twenty-first century. Owing partly to unclear contributions of microbial processes to NO_x emissions, many countries have been engaging in developing technologies and measures for reducing fossil-fuel NO_x emissions to reduce airborne and water N pollution, with a focus on adjusting energy systems and increasing the chemical conversion of NO_x to reduce emissions during fossil-fuel combustion. Our findings point to the need to consider the substantial contribution of the microbial N cycle to atmospheric NO_x loadings while reducing fossil-fuel NO_x emissions. Accordingly, the potential costs and impacts of reducing fossil-fuel NO_x emissions need to be re-assessed when making more effective emission mitigation strategies—including the indirect effects of anthropogenic N on terrestrial and marine microbial processes. Moreover, the isotopically constrained microbial NO_x emissions and updated total NO_x emissions we provide are helpful for benchmarking atmospheric and earth system models that project the feedback between the biosphere, climate and global N cycle.

In summary, based on large-scale isotope observations of p-NO_3^- in the atmosphere, we established a simple but effective approach for estimating NO_x sources in the atmosphere. Before, isotope mass-balance models have been constructed to successfully partition continental hydrologic fluxes and quantify the contributions of local evaporation and ocean-to-land water transportation to the land moisture [92,93]. Accordingly, the framework established in our study enriches the application of isotopic mass-balance approaches in quantifying processes and fluxes of global biogeochemical cycles. However, our method can only consider dominant sources of NO_x emissions. Additional work on detailed measurements of $\delta^{15}N$ values for all NO_x emission sources could further refine our estimates. Isotope observations of p-NO_3^- in the atmosphere across more sampling areas will be critical to reducing uncertainties in our estimation and offering spatial tools to pinpoint source regions of great concern.

MATERIALS AND METHODS

Detailed materials and methods are given in the online supplementary materials.

SUPPLEMENTARY DATA

Supplementary data are available at *NSR* online.

ACKNOWLEDGEMENTS

We thank all researchers who reported and kindly provided us with precious data on concentrations and isotopes of atmospheric NO_y.

FUNDING

This work was supported by the National Natural Science Foundation of China (42125301, 41730855 and 42073005) and the Coordinated Research Project of IAEA (F32008).

AUTHOR CONTRIBUTIONS

X.Y.L. designed the research. W.S. and X.Y.L. conducted the research (data collections and analyses). W.S. and X.Y.L. co-wrote the paper. B.Z.H. and C.Q.L. commented on the manuscript.

Conflict of interest statement. None declared.

REFERENCES

1. Davidson EA, David MB and Galloway JN *et al.* Excess nitrogen in the US environment: trends, risks, and solutions. *Issues Ecol* 2012; **15**: 1–16.
2. Lerdau MT, Munger JW and Jacob DJ. The NO_2 flux conundrum. *Science* 2000; **289**: 2291–3.
3. Beirle S, Boersma KF and Platt U *et al.* Megacity emissions and lifetimes of nitrogen oxides probed from space. *Science* 2011; **333**: 1737–9.
4. Mushinski RM, Phillips RP and Payne ZC *et al.* Microbial mechanisms and ecosystem flux estimation for aerobic NO_y emissions from deciduous forest soils. *Proc Natl Acad Sci USA* 2019; **116**: 2138–45.
5. Keeler BL, Gourevitch JD and Polasky S *et al.* The social costs of nitrogen. *Sci Adv* 2016; **2**: e1600219.
6. Galloway JN, Dentener FJ and Capone DG *et al.* Nitrogen cycles: past, present, and future. *Biogeochemistry* 2004; **70**: 153–226.
7. Fowler D, Coyle M and Skiba U *et al.* The global nitrogen cycle in the twenty-first century. *Phil Trans R Soc B* 2013; **368**: 20130164.
8. Liu XJ, Zhang Y and Han WX *et al.* Enhanced nitrogen deposition over China. *Nature* 2013; **494**: 459–62.
9. Clark CM and Tilman D. Loss of plant species after chronic low-level nitrogen deposition to prairie grasslands. *Nature* 2008; **451**: 712–5.
10. Sutton MA, Oenema O and Erisman JW *et al.* Too much of a good thing. *Nature* 2011; **472**: 159–61.
11. Bautres M, Drake TW and Verbeeck H *et al.* High fire-derived nitrogen deposition on central African forests. *Proc Natl Acad Sci USA* 2018; **115**: 549–54.
12. Chen J, Luo YQ and Groenigen KJV *et al.* A keystone microbial enzyme for nitrogen control of soil carbon storage. *Sci Adv* 2018; **4**: eaaq1689.
13. Hall SJ and Matson PA. Nitrogen oxide emissions after nitrogen additions in tropical forests. *Nature* 1999; **400**: 152–5.
14. Corbett JJ and Koehler HW. Updated emissions from ocean shipping. *J Geophys Res* 2003; **108**: 4650.
15. Eyring V, Köhler HW and Aardenne JV *et al.* Emissions from international shipping: 1. The last 50 years. *J Geophys Res* 2005; **110**: D17305.
16. Eyring V, Isaksen ISA and Berntsen T *et al.* Transport impacts on atmosphere and climate: shipping. *Atmos Environ* 2010; **44**: 4735–71.
17. Holmes CD, Prather M and Vinken GCM. The climate impact of ship NO_x emissions: an improved estimate accounting for plume chemistry. *Atmos Chem Phys* 2014; **14**: 6801–12.
18. Yan F, Winijkul E and Streets DG *et al.* Global emission projections for the transportation sector using dynamic technology modeling. *Atmos Chem Phys* 2014; **14**: 5709–33.
19. Johansson L, Jalkanen JP and Kukkonen J. Global assessment of shipping emissions in 2015 on a high spatial and temporal resolution. *Atmos Environ* 2017; **167**: 403–15.
20. Jonson JE, Gauss M and Schulz M *et al.* Effects of global ship emissions on European air pollution levels. *Atmos Chem Phys* 2020; **20**: 11399–422.
21. Zafiriou OC, McFarland M and Bromund RH. Nitric oxide in seawater. *Science* 1980; **207**: 637–9.
22. Ward BB and Zafiriou OC. Nitrification and nitric oxide in the oxygen minimum of the eastern tropical north pacific. *Deep Sea Res Part I* 1988; **35**: 1127–42.
23. Liu CY, Zhao M and Ren CY *et al.* Direct measurement of nitric oxide in seawater medium by fluorometric method. *Chin J Anal Chem* 2009; **37**: 1463–7.
24. Lutterbeck HE and Bange HW. An improved method for the determination of dissolved nitric oxide (NO) in seawater samples. *Ocean Sci* 2015; **11**: 937–46.
25. Firestone MK, Firestone RB and Tiedje JM. Nitric oxide as an intermediate in denitrification: evidence from nitrogen-13 isotope exchange. *Biochem Biophys Res Commun* 1979; **91**: 10–6.
26. Lipschultz F, Zafiriou OC and Wofsy SC *et al.* Production of NO and N_2O by soil nitrifying bacteria. *Nature* 1981; **294**: 641–3.
27. Yoshinari T. Nitrite and nitrous oxide production by *Methylosinus trichosporium*. *Can J Microbiol* 1985; **31**: 139–44.
28. Freitag A and Bock E. Energy conservation in Nitrobacter. *FEMS Microbiol Lett* 1990; **66**: 157–62.
29. Thamdrup B. New pathways and processes in the global nitrogen cycle. *Annu Rev Ecol Evol Syst* 2012; **43**: 407–28.
30. Schreiber F, Polerecky L and de Beer D. Nitric oxide microsensor for high spatial resolution measurements in biofilms and sediments. *Anal Chem* 2008; **80**: 1152–8.
31. Wang KK, Tian Y and Li PF *et al.* Sources of nitric oxide during the outbreak of Ulva prolifera in coastal waters of the Yellow Sea off Qingdao. *Mar Environ Res* 2020; **162**: 1–10.
32. Williams JE, Bras GL and Kukui A *et al.* The impact of the chemical production of methyl nitrate from the $NO+CH_3O_2$ reaction on the global distributions of alkyl nitrates, nitrogen oxides and tropospheric ozone: a global modelling study. *Atmos Chem Phys* 2014; **14**: 2363–82.
33. Fisher JA, Atlas EL and Barletta B *et al.* Methyl, ethyl, and propyl nitrates: global distribution and impacts on reactive nitrogen in remote marine environments. *J Geophys Res Atmos* 2018; **123**: 12429–51.
34. Alexander B, Sherwen T and Holmes CD *et al.* Global inorganic nitrate production mechanisms: comparison of a global model with nitrate isotope observations. *Atmos Chem Phys* 2020; **20**: 3859–77.
35. Altieri KE, Fawceet SE and Hastings MG. Reactive nitrogen cycling in the atmosphere and ocean. *Annu Rev Earth Planet Sci* 2021; **49**: 523–50.
36. Schreiber F, Wunderlin P and Udert KM *et al.* Nitric oxide and nitrous oxide turnover in natural and engineered microbial communities: biological pathways, chemical reactions, and novel technologies. *Front Microbio* 2012; **3**: 372.
37. Richter A, Burrows JP and Nüß H *et al.* Increase in tropospheric nitrogen dioxide over China observed from space. *Nature* 2005; **437**: 129–32.
38. Kampschreur MJ, Star WRL and Wielders HA *et al.* Dynamics of nitric oxide and nitrous oxide emission during full-scale reject water treatment. *Water Res* 2008; **42**: 812–26.
39. Pocquet M, Wu Z and Queinnec I *et al.* A two pathway model for N_2O emissions by ammonium oxidizing bacteria supported by the NO/N_2O variation. *Water Res* 2016; **88**: 948–59.
40. Almaraz M, Bai E and Wang C *et al.* Agriculture is a major source of NO_x pollution in California. *Sci Adv* 2018; **4**: eaao3477.
41. Streets DG, Yarber KF and Woo JH *et al.* Biomass burning in Asia: annual and seasonal estimates and atmospheric emissions. *Glob Biogeochem Cycle* 2003; **17**: 1099.
42. Oberschelp C, Pfister S and Raptis C *et al.* Global emission hotspots of coal power generation. *Nat Sustain* 2019; **2**: 113–21.
43. Jaeglé L, Steinberger L and Martin RV *et al.* Global partitioning of NO_x sources using satellite observations: relative roles of fossil fuel combustion, biomass burning and soil emissions. *Farad Discuss* 2005; **130**: 407–23.
44. Jain AK, Tao ZN and Yang XJ *et al.* Estimates of global biomass burning emissions for reactive greenhouse gases (CO, NMHCS, and NO_x) and CO_2. *J Geophys Res* 2006; **111**: D06304.

45. European Environment Agency. *National Emission Ceilings Directive emissions data viewer 1990–2017*. https://www.eea.europa.eu/data-and-maps/dashboards/necd-directive-data-viewer-2 (5 July 2022, date last accessed).
46. Government of Canada. *Air Pollutant and Black Carbon Emissions Inventories online search*. https://pollution-waste.canada.ca/air-emission-inventory (5 July 2022, date last accessed).
47. United States Environmental Protection Agency. *Air Pollutant Emissions Trends Data*. https://www.epa.gov/air-emissions-inventories/air-pollutant-emissions-trends-data (5 July 2022, date last accessed).
48. Oikawa PY, Ge C and Wang J *et al.* Unusually high soil nitrogen oxide emissions influence air quality in a high-temperature agricultural region. *Nat Commun* 2015; **6**: 8753.
49. IPCC: Climate Change 2001: *Synthesis Report: Contribution of Working Groups I, II, and III to the Third Assessment Report of the Intergovernmental Panel on Climate Change*, edited by Watson RT, Albritton DL and Barker T *et al.* Cambridge: Cambridge University Press, 2001, 1–397.
50. IPCC: Climate Change 2013: *Carbon and Other Biogeochemical Cycles: Contribution of Working Group I to the Fifth Assessment Report of the Intergovernmental Panel on Climate Change*, edited by Ciais P, Sabine C and Bala G *et al.* Cambridge: Cambridge University Press, 2013, 465–570.
51. Oki T and Kanae S. Global hydrological cycles and world water resources. *Science* 2006; **313**: 1068–72.
52. Abbott BW, Bishop K and Zarnetske JP *et al.* Human domination of the global water cycle absent from depictions and perceptions. *Nat Geosci* 2019; **12**: 533–40.
53. McElroy MB and Wang YX. Human and animal wastes: implications for atmospheric N_2O and NO_x. *Glob Biogeochem Cycle* 2005; **19**: GB2008.
54. Steinkamp J, Ganzeveld LN and Wilcke W *et al.* Influence of modelled soil biogenic NO emissions on related trace gases and the atmospheric oxidizing efficiency. *Atmos Chem Phys* 2009; **9**: 2663–77.
55. Miyazaki, Eskes H and Sudo K *et al.* Decadal changes in global surface NO_x emissions from multi-constituent satellite data assimilation. *Atmos Chem Phys* 2017; **17**: 807–37.
56. Huang TB, Zhu X and Zhong QR *et al.* Spatial and temporal trends in global emissions of nitrogen oxides from 1960 to 2014. *Environ Sci Technol* 2017; **51**: 7992–8000.
57. Geddes JA and Martin RV. Global deposition of total reactive nitrogen oxides from 1996 to 2014 constrained with satellite observations of NO_2 columns. *Atmos Chem Phys* 2017; **17**: 10071–91.
58. Qu Z, Henze DK and Cooper OR *et al.* Impacts of global NO_x inversions on NO_2 and ozone simulations. *Atmos Chem Phys* 2020; **20**: 13109–30.
59. Beirle S, Platt U and Wenig M *et al.* Highly resolved global distribution of tropospheric NO_2 using GOME narrow swath mode data. *Atmos Chem Phys* 2004; **4**: 1913–24.
60. Elshorbany YF, Crutzen PJ and Steil B *et al.* Global and regional impacts of HONO on the chemical composition of clouds and aerosols. *Atmos Chem Phys* 2014; **14**: 1167–84.
61. Tan JN, Fu JS and Dentener F *et al.* Multi-model study of HTAP II on sulfur and nitrogen deposition. *Atmos Chem Phys* 2018; **18**: 6847–66.
62. Jickells TD, Buitenhuis E and Altieri K *et al.* A reevaluation of the magnitude and impacts of anthropogenic atmospheric nitrogen inputs on the ocean. *Glob Biogeochem Cycle* 2017; **31**: 289–305.
63. Morin S, Savarino J and Frey MM *et al.* Tracing the origin and fate of NO_x in the arctic atmosphere using stable isotopes in nitrate. *Science* 2008; **322**: 730–2.
64. Altieri KE, Hastings MG and Peter AJ *et al.* Isotopic evidence for a marine ammonium source in rainwater at Bermuda. *Glob Biogeochem Cycle* 2014; **28**: 1066–80.
65. Song W, Liu XY and Liu CQ. New constraints on isotopic effects and major sources of nitrate in atmospheric particulates by combining $\delta^{15}N$ and $\Delta^{17}O$ signatures. *J Geophys Res-Atmos* 2021; **126**: e2020JD034168.
66. Price C, Penner J and Prather M. NO_x from lightning, global distribution based on lightning physics. *J Geophys Res* 1997; **102**: 5929–41.
67. Li ZJ, Hasting MG and Walters WW *et al.* Isotopic evidence that recent agriculture overprints climate variability in nitrogen deposition to the Tibetan Plateau. *Environ Int* 2020; **138**: 105614.
68. Walters WW and Michalski G. Theoretical calculation of nitrogen isotope equilibrium exchange fractionation factors for various NO_y molecules. *Geochim Cosmochim Acta* 2015; **164**: 284–97.
69. Walters WW and Michalski G. Theoretical calculation of oxygen equilibrium isotope fractionation factors involving various NO_y molecules, radical OH, and H_2O and its implications for isotope variations in atmospheric nitrate. *Geochim Cosmochim Acta* 2016; **191**: 89–101.
70. Dentener F, Stevenson D and Ellingsen K *et al.* The global atmospheric environment for the next generation. *Environ Sci Technol* 2006; **40**: 3586–94.
71. Vuuren DPV, Bouwman LF and Smith SJ *et al.* Global projections for anthropogenic reactive nitrogen emissions to the atmosphere: an assessment of scenarios in the scientific literature. *Curr Opin Environ Sustain* 2011; **3**: 359–69.
72. Lamsal LN, Martin RV and Padmanabhan A *et al.* Application of satellite observations for timely updates to global anthropogenic NO_x emission inventories. *Geophys Res Lett* 2011; **38**: L05810.
73. Gu D, Wang YH and Smeltzer C *et al.* Anthropogenic emissions of NO_x over China: reconciling the difference of inverse modeling results using GOME-2 and OMI measurements. *J Geophys Res Atmos* 2014; **119**: 7732–40.
74. Marais EA, Jacob DJ and Choi S *et al.* Nitrogen oxides in the global upper troposphere: interpreting cloud-sliced NO_2 observations from the OMI satellite instrument. *Atmos Chem Phys* 2018; **18**: 17017–27.
75. Müller JF. Geographical distribution and seasonal variation of surface emissions and deposition velocities of atmospheric trace gases. *J Geophys Res* 1992; **97**: 3787–804.
76. Yienger JJ and Levy H II. Empirical model of global soil-biogenic NO_x emissions. *J Geophys Res* 1995; **100**: 11447–64.
77. Ganzeveld LN, Lelieveld J and Dentener FJ *et al.* Global soil-biogenic NO_x emissions and the role of canopy processes. *J Geophys Res* 2002; **107**: 9–17.
78. Yan XY, Ohara T and Akimoto H. Statistical modeling of global soil NO_x emissions. *Glob Biogeochem Cycle* 2005; **19**: GB3019.
79. Stavrakou T, Müller JF and Boersma KF *et al.* Assessing the distribution and growth rates of NO_x emission sources by inverting a 10-year record of NO_2 satellite columns. *Geophys Res Lett* 2008; **35**: L10801.
80. Stavrakou T, Müller JF and Boersma KF *et al.* Key chemical NO_x sink uncertainties and how they infuence top-down emissions of nitrogen oxides. *Atmos Chem Phys* 2013; **13**: 9057–82.
81. Steinkamp J and Lawrence MG. Improvement and evaluation of simulated global biogenic soil NO emissions in an AC-GCM. *Atmos Chem Phys* 2011; **11**: 6063–82.
82. Hudman RC, Moore NE and Mebust AK *et al.* Steps towards a mechanistic model of global soil nitric oxide emissions: implementation and space based constraints. *Atmos Chem Phys* 2012; **12**: 7779–95.
83. Heald CL and Geddes JA. The impact of historical land use change from 1850 to 2000 on secondary particulate matter and ozone. *Atmos Chem Phys* 2016; **16**: 14997–5010.

84. Weng HJ, Lin JT and Martin R *et al.* Global high-resolution emissions of soil NO_x, sea salt aerosols, and biogenic volatile organic compounds. *Sci Data* 2020; **7**: 148.
85. Wang C, Houlton BZ and Dai WW *et al.* Growth in the global N_2 sink attributed to N fertilizer inputs over 1860 to 2000. *Sci Total Environ* 2017; **574**: 1044–53.
86. Müller JF and Stavrakou T. Inversion of CO and NO_x emissions using the adjoint of the IMAGES model. *Atmos Chem Phys* 2005; **5**: 1157–86.
87. Vinken GCM, Boersma KF and Maasakkers JD *et al.* Worldwide biogenic soil NO_x emissions inferred from OMI NO_2 observations. *Atmos Chem Phys* 2014; **14**: 10363–81.
88. Dentener F, Drevet J and Lamarque JF *et al.* Nitrogen and sulfur deposition on regional and global scales: a multimodel evaluation. *Glob Biogeochem Cycle* 2006; **20**: GB4003.
89. Duce RA, Laroche J and Altieri K *et al.* Impacts of atmospheric anthropogenic nitrogen on the open ocean. *Science* 2008; **320**: 893–7.
90. Vet R, Artz RS and Carou S *et al.* A global assessment of precipitation chemistry and deposition of sulfur, nitrogen, sea salt, base cations, organic acids, acidity and pH, and phosphorus. *Atmos Environ* 2014; **93**: 3–100.
91. Weber B, Wu DM and Alexandra T *et al.* Biological soil crusts accelerate the nitrogen cycle through large NO and HONO emissions in drylands. *Proc Natl Acad Sci USA* 2015; **112**: 15384–9.
92. Worden J, Noone D and Bowman K *et al.* Importance of rain evaporation and continental convection in the tropical water cycle. *Nature* 2007; **455**: 528–32.
93. Good SP, Noone D and Bowen G. Hydrologic connectivity constrains partitioning of global terrestrial water fluxes. *Science* 2015; **349**: 175–7.